Mem. Natl Inst. Polar Res., Spec. Issue, **54**, 193–201, 2001

Scientific note

Effects on spectral reflectance from snow ageing

J-G. Winther[1], S. Gerland[1,3], J. B. Ørbæk[1], B. Ivanov[2], A. S. Zachek[2] and A. M. Bezgreshnov[2]

[1]*Norwegian Polar Institute, Polar Environmental Centre, N-9296 Tromsø, Norway (corresponding author's E-mail: winther@npolar.no)*
[2]*Arctic and Antarctic Research Institute, Bering 38, 199397 St. Petersburg, Russia*
[3]*Present address: Norwegian Radiation Protection Authority, Polar Environmental Centre, N-9296 Tromsø, Norway*

Abstract: This scientific note elaborates on the role that snow plays as an insulator for solar radiation on Arctic tundra and sea ice. We present spectral radiation data on i) surface reflectance, ii) attenuation in snow packs on land and on sea ice, and iii) under-ice irradiance. Our data is collected at Arctic tundra and fast-ice sites on Svalbard and in the Pechora Sea during spring melt-conditions. Although the spectrally-integrated surface reflectance, or albedo, decreases relative steadily in spring, we find that the infrared (IR) albedo decreases most strongly in the initial phase of snow melt while the visible albedo drops more quickly later on. The fact that the spectral signature of snow changes with time put restrictions on obtaining accurate satellite-derived narrow-band albedo measurements; however, new sensors will introduce significant improvements. Although thin, the presence of a snow cover fully dominates the exchange of solar radiation between the atmosphere and the sea ice-ocean system. Thus, a changing precipitation pattern (in time and space) in the Arctic Ocean can play a crucial role on sea-ice thickness distribution in a climate warming scenario. At last, this work suggests that the parameterisation of albedo in climate models could attempt to describe optical characteristics more realistically.

1. Introduction

The classical model work of Wiscombe and Warren (1980), Warren and Wiscombe (1980) and Warren (1982) thoroughly discusses the various factors affecting the albedo, such as snow depth, grain size, liquid water content, incident angle, and contamination. Later, a wide variety of field measurements and other theoretical studies of these relationships have been reported (*e.g.* Gerland *et al.*, 1999a,b; Grenfell *et al.*, 1981, 1994; Hall *et al.*, 1995; Knap and Reijmer, 1998; Liston, 1995; Perovich *et al.*, 1998; Steffen and Heinrichs, 1994; Winther *et al.*, 1999). Hence, during the last two decades we have gained a substantial knowledge on the reflective characteristics of snow.

Surface albedo is known to be one of the key parameters in the climate system in polar regions and very important in feedback processes (Curry *et al.*, 1995; IPCC TAR, in press). Obviously, a complicating factor for precise representation of snow cover and sea ice in large-scale models such as General Circulation Models (GCMs) is the extreme sub-grid

scale variability that occurs (Barry, 1996). Today, some GCMs make use of a time-dependent decay of snow albedo. Recent experiments with the ECHAM GCM have revealed that substantial improvement in the representation of snow albedo can be achieved when the shortwave albedo is treated separately in two bands, split at 700 nm (Ohmura, pers. commun., 2000). Therefore, it seems timely to utilise the detailed knowledge achieved in the previously-mentioned studies for improving the parameterisation of albedo in climate models. Furthermore, new generation satellite instruments, *e.g.* ESA's Envisat MERIS sensor, will enable us to measure spectral reflectance (in time and space) more accurately in future and they can provide improved input data for climate simulations. Also, in addition to being important for the surface energy-balance, attenuation of solar radiation determines how much radiation that is available for biological activity at the beginning of the growth season (*e.g.* for *collembola,* plants, moss, and lichen).

In this scientific note, we present data that illuminates various aspects of the reflection and attenuation behaviour of snow and sea ice. These examples are used in the following discussion where we indicate some future challenges concerning utilising information on spectral reflectance in climatic research.

2. Spectral reflectance measurements

2.1. Surface reflectance of melting snow at a tundra site

Figure 1 presents spectral reflectance from a tundra site near Ny-Ålesund at about 79°N on Svalbard for snow of various degrees of metamorphosis, surface blackening, and snow pack thickness measured in spring 1997. The data has been acquired by use of a FieldSpec spectroradiometer (Winther *et al.*, 1999). Curve 1 was acquired on 19 of May (clear skies) and represents dry, uncontaminated snow that had undergone minor metamorphosis. Curves 2 and 3 were taken on melting snow on June 8 and June 13, respectively (both cloudy days). By comparing Curves 2 and 3, it becomes clear that the decrease in reflectance is more pronounced in the near infrared (NIR) wavelength region than in the visible (VIS). This is partly caused by snow-grain growth. However, maybe more important is the increasing liquid-water content that replaces air with water between the ice grains. Then, because the spectral refractive index of liquid water is very close to that of ice for these wavelengths, the effective grain-size increases, and is followed by a decreasing reflectance. On contrary, the drop in reflectance in the VIS is more prominent than in the NIR between 13 and 19 of June (between Curve 3 and Curves 4 and 5) due to increasing surface blackening, mainly by local organic material transported from nearby snow-free areas as the snow cover depletes.

Curve 5 (cloudy) was acquired on a site in which a thin snow layer of 0.5 to 3 cm covered a 5–10 cm ice layer lying over the ground, with some free water present at the ice-soil interface. The low reflectance, in particular in the VIS region, is mainly caused by the thin layers of snow and ice covering the ground. In addition, the surface was strongly blackened by soil particles at this site. Curve 6 was measured over bare tundra.

Albedo is measured routinely at a nearby research station. Albedo is the spectral directional-hemispherical reflectance, *i.e.* it is the integral of reflectance over all (shortwave) wavelengths and reflection angles (Warren, 1982). For 19 of May, 8, 13, and 19 of June these values were 0.78, 0.76, 0.70, and 0.32, respectively. These values are marked as — on Fig. 1.

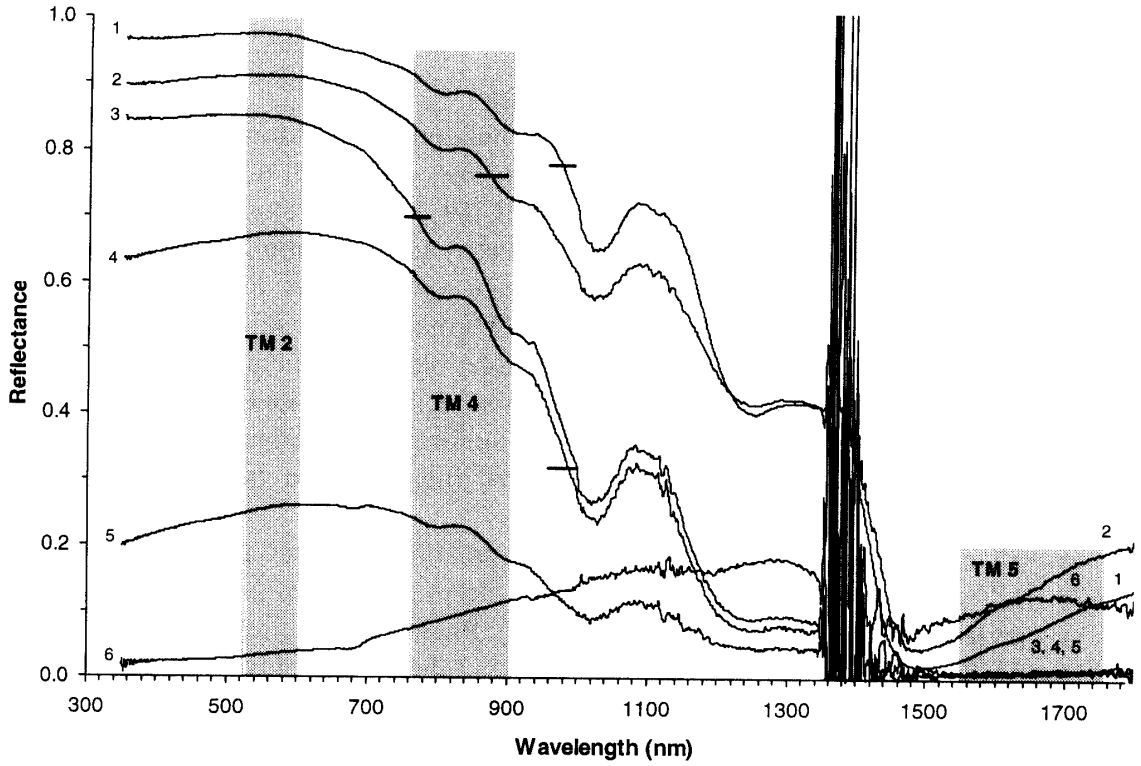

Fig. 1. Examples showing reflectance of snow with various degrees of metamorphosis, surface blackening, and snow pack thickness from Ny-Ålesund, Svalbard, in 1997. Curve 1 was acquired on May 19 (clear skies) and represents dry snow (snow thickness, s_h, = 45 cm) that had undergone minor metamorphosis and with an apparently unpolluted surface. Curves 2 and 3 were taken at melting snow surfaces on 8 and 13 of June, respectively (cloudy; s_h = 39 cm and 24 cm, respectively). Curves 4–6 were measured on 19 of June (cloudy). Curve 4 represents snow that had undergone about one month of snow metamorphosis and with some surface blackening (s_h = 5 cm). Curve 5 was acquired on a site where a thin snow layer of 0.5 to 3 cm covered a 5–10 cm thick ice layer sheltering the ground. In addition, the surface was strongly blackened by soil particles at this site. Curve 6 was measured over bare tundra. Spectrally-integrated albedo values from the nearby long-term albedo measuring site from 19 of May, 8, 13, and 19 of June, respectively, are marked on the figure as —. Finally, the wavelength ranges (or bands) covered by Landsat TM Bands 2, 4, and 5 are shown (from Winther et al., 1999). The small difference in reflectance between Curves 1 and 2 (dry snow < melting snow) is probably caused by different cloud conditions. The solar zenith angle was similar on these two days (~60 degrees).

The spectrally-integrated reflectance is, of course, often the most interesting figure for hydrological applications, *e.g.* for calculation of melt rates. Figure 1 shows that for the specific situation occurring in spring 1997, satellite-derived albedo in the NIR as measured, for example by Landsat TM Band 4, would in most cases yield slightly higher albedo estimates than the spectrally-integrated reflectance (285–2800 nm). However, important to notice here is that the variable spectral signature of melting snow makes it inappropriate to use one fixed satellite band throughout the melt season to acquire precise satellite-derived estimates of albedo. It should be noted that the large fluctuations around 1400 and 1800 nm are caused by the very small downward solar flux due to atmospheric absorption at these

wavelengths, *i.e.* a small signal to noise ratio.

2.2. Attenuation of radiation in a tundra snow pack

Figure 2 shows measured and modelled attenuation of radiation in a tundra snow pack before and after onset of melt. Measurements are obtained in the spring seasons of 1997 and 1998 in Ny-Ålesund using a Licor LI-189 PAR (Photosynthetically Active Radiation) quantum-meter along with snow parameters such as density, grain size, content of liquid water, temperature, thickness, and stratification (Gerland *et al.*, 2000). The model used is a two-stream 1-D model (Liston *et al.*, 1999) that is based on works by Schlatter (1972) and Brandt and Warren (1993). It can be used both with a constant or a variable extinction coefficient. Model input are snow grain-size, density, surface and soil albedo, and the spectrum of solar radiation as measured at the surface. Output from the model consists of downward and upward fluxes for 5000 layers, including the calculated extinction coefficient.

Overall, and in accordance with theory, solar radiation penetrates more efficiently into a snow pack after it has begun to melt since the effective grain-size increases when water becomes present, thus reducing the albedo (Fig. 2). Reasons for the relatively high degree of scatter in the measured data are mainly because i) they were collected throughout the

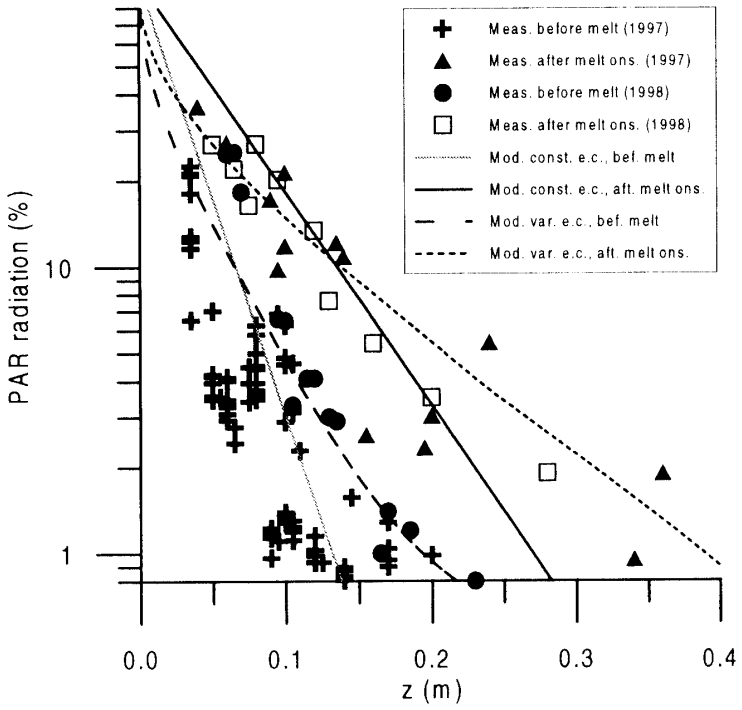

Fig. 2. In-situ attenuation-measurements of PAR and model simulations. Data is collected from various snow pits at Ny-Ålesund, Svalbard, before and after the onset of melt. The relative instrument reading Q(z)/Q(surface) is plotted at logarithmic scale versus snow thickness z above sensor. Model simulations are displayed for runs using constant and variable extinction-coefficients. Clearly, it can be seen that the snow pack becomes more transparent to solar radiation after the onset of melt (modified after Gerland et al., 2000).

melt period, *i.e.* over a time period when the snow pack gradually changed from dry to fully isothermal, and therefore the portion of the snow pack containing liquid water varied and ii) no distinguishing between measurements made under overcast or clear skies were made. It is known that the spectral composition of solar radiation received by a surface changes substantially during cloudy conditions since clouds absorb more of the infrared radiation than of the visible. Also, model simulations deviate somewhat from field measurements. We think this mainly is caused by a discrepancy between observed grain size (too large) and the real (optically) grain size where sub-grain size structures and non-spherical forms are important for scattering incidences to occur while these sub-structures are difficult to register by field methods (magnifying glass) (Grenfell and Warren, 1999).

2.3. Surface reflectance and under-ice irradiance of a fast-ice cover

Figure 3a shows surface albedo on a fast ice location in Kongsfjorden, Svalbard, for three stages in the development of snow melt during spring 1997 (Gerland *et al.*, 1999a). On 18 of May, the snow and sea-ice thickness were 20 cm and 70 cm, respectively. Average snow-density and grain-size were 318 kg/m^3 and 2 mm; the snow pack was dry. On 3 of June, the average density and snow grain size had increase to 356 kg/m^3 and 4 mm, respectively. However, the surface was covered by a thin layer of fresh snow with an observed grain size of 0.5 mm. The layer of freshly-fallen snow is the reason why the observed decrease in reflectance between 18 of May and 3 of June affects the visible albedo only (Fig. 3a). The explanation can be found in the fact that visible radiation penetrates deeper (*i.e.,* through the thin top-layer of snow) than infrared radiation does. The increased average grain-size decreases the visible albedo because the snow pack becomes more transparent and affected by the underlying sea ice whereas this does not happen in the infrared region where the thin, fresh snow-layer blocks out the IR radiation. Later, however, the fresh snow-layer thaws and then we experience a more pronounced decrease in the IR region. On 18 of June 1997, melting reached an advanced stage and only a little snow was left. Snow grains reached sizes of 5 to 10 mm, the surface was wet and melt ponds developed.

Figure 3b presents an experiment where irradiance was measured under the fast ice; first for an undisturbed situation and later for a sea-ice surface that had been cleared for snow. Thus, this enabled us to distinguish between the attenuation effect from sea ice only and from the original combined ice and snow-layer situation. The snow cover had a thickness of 21 cm, a temperature of -2.8°C, an average density of 260 kg/m^3, and with grain sizes varying from 0.1 to 5 mm (smallest grains at the top). Clearly seen on Fig. 3b, only about 1% of the irradiance at 550 nm reaches the water masses compared to the irradiance at the surface in the undisturbed case. After snow has been removed, about 27 times more solar radiation at 550 nm penetrates the sea ice and is thus received by the water masses beneath it. This relation factor is even higher for shorter and longer wavelengths.

2.4. Attenuation of radiation in snow that covers sea ice

An adequate understanding of shortwave radiative interactions in an atmosphere-sea ice-ocean system is critical for addressing issues such as sea-ice melt-rates, upper-ocean stratification processes, biological productivity-levels, as well as surface energy and mass-balance budget-calculations. Contrary to fast ice, pack ice is highly heterogeneous on

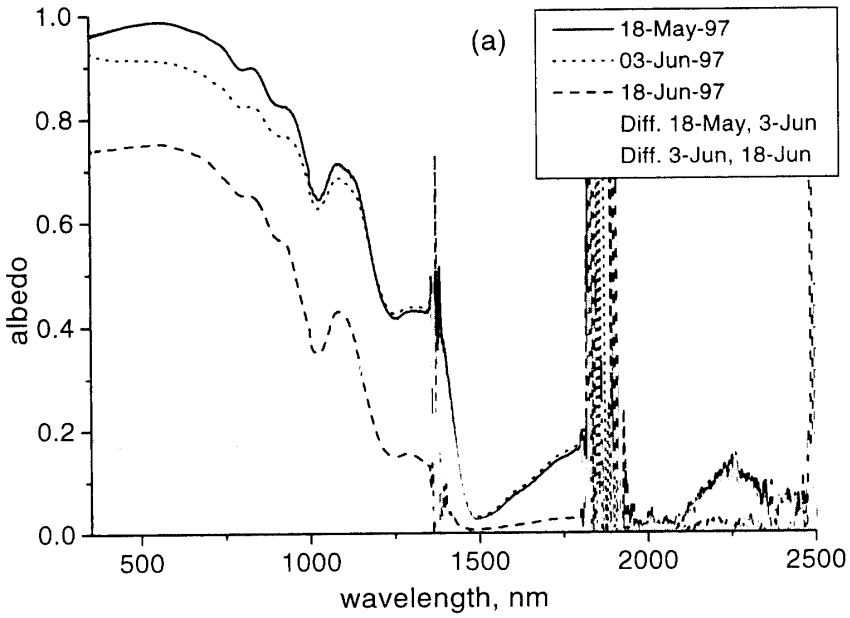

Fig. 3a. Surface reflectance from early-, mid-, and late spring season in 1997 over snow- covered sea ice in Kongsfjorden, Svalbard. Also plotted is the difference in albedo between 18 of May and 3 of June and between 3 of June and 18 of June. Note that the decrease in albedo appears in the visible region for the first period and to a larger extent in the infrared region for the latter.

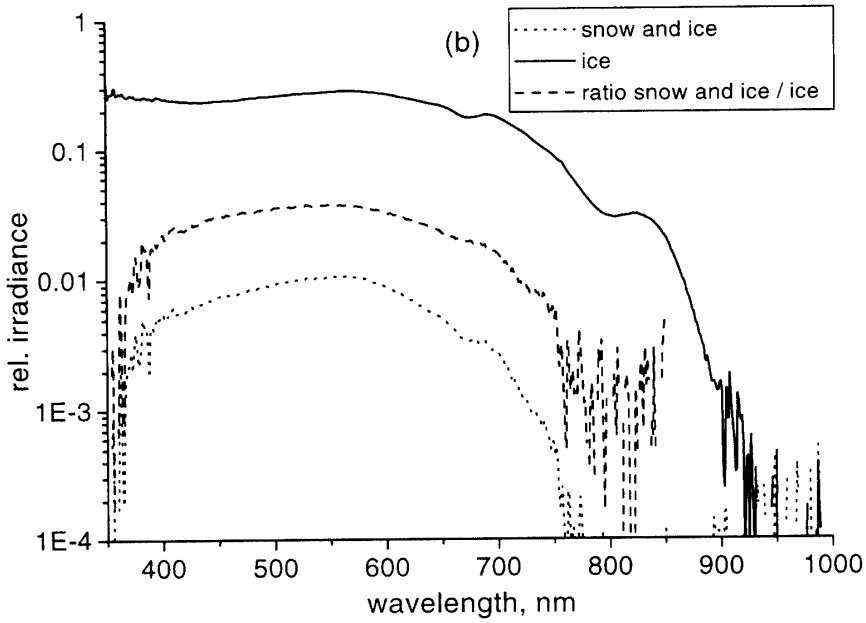

Fig. 3b. Under-ice irradiance measurements on fast ice in Kongsfjorden were acquired on 13 of May 1998. Spectral irradiance that reaches the water masses is plotted in percentage of the irradiance at the surface with and without snow on top of the sea ice (solid curve; snow was removed) (after Gerland et al., 1999a). It was stable, clear skies conditions on all observation days.

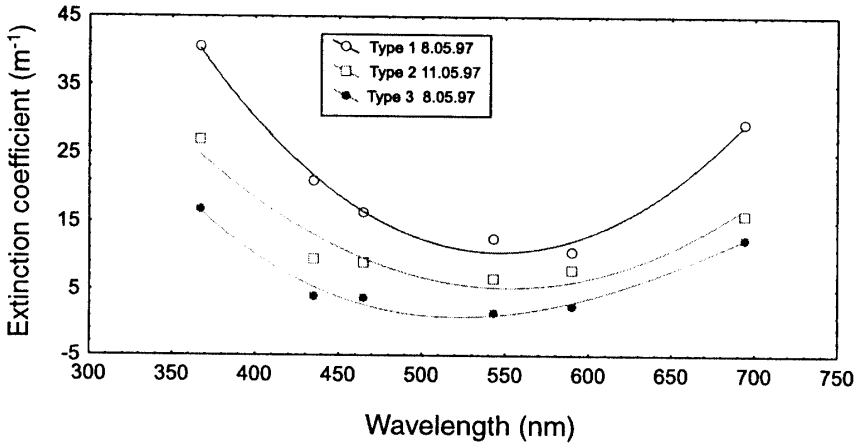

Fig. 4. Index for attenuation of irradiance in three different snow packs (all three were melting snow packs; other information n.a.) covering sea ice in the Pechora Sea, May 1997. Naturally, least attenuation is found in the central parts of the photosynthetic active region (around 550 nm) which also corresponds with under-ice measurements made on Svalbard (Fig. 3b).

horizontal scales of tens of meters due to the dynamic behaviour of drifting ice. Thus, the amount of solar radiation absorbed by the sea ice-ocean system is largely dependent on parameters such as brine volume, air-bubble distribution, ice thickness, presence of melt ponds, as well as snow-cover distribution and its characteristics.

Here, we only address one part of this extremely complex and highly varying system, namely the spectral extinction-coefficient of snow. Figure 4 shows how the PAR has attenuated at a fixed depth for three locations at 8 and 11 of May 1997 in the Pechora Sea. The largest penetration, or weakest attenuation, occurs in the central part of the PAR region at about 550 nm. This corresponds very well with under-ice irradiance measurements from Svalbard (Fig. 3b) showing that radiation at about 550 nm penetrates the snow-sea ice system most efficiently (*i.e.*, the curves in Figs. 3b and 4 have opposite curvatures). Another thing worthwhile mentioning is that relative large differences in attenuation occur over narrow wavelength-ranges, thus measurements by instruments averaging over broad bands will not detect these variations adequately. This has relevance for satellite-derived albedo measurements where the relative coarse spectral resolution of sensors often smooth out some of the spectral details present. Finally, a change of seasonal snow-characteristics as would happen in a warming scenario would have important impacts on the attenuation of solar radiation in snow packs, both in a terrestrial (Fig. 2) and marine environment (Fig. 4), with consequences on biological productivity.

3. Discussion and outlook

Our data shows that measurements of snow albedo, *i.e.* spectrally-integrated reflectance, using a narrow-band albedo as an indicator of shortwave albedo has severe weaknesses. This approach is commonly used in satellite remote-sensing studies but works inappropriately for melting snow because the spectral signature changes considerably

during the melt season. New sensors such as the NASA's Terra MODIS (launched in December 1999) and ESA's Envisat MERIS (launch planned in summer 2001) have a wide range of narrow bands and thus represent improved tools for accurate monitoring of broad-band albedo when combining various narrow satellite-bands.

In the beginning of the melt season the albedo drops fastest in the NIR region on tundra snow due to the increasing effective grain-size caused by the presence of liquid water and general metamorphosis of snow. Later, the VIS albedo reduction dominates due to contamination of the surface and a thinning snow pack. Interestingly, for one incident where fresh snow fell after the onset of melt, the reversed tendency happened over snow-covered fast ice on Kongsfjorden, Svalbard. Here, the initial snow cover was thin (about 20 cm). Thus, the underlying darker sea ice affected the visible surface albedo quickly after the onset of melt. Later on, the reduction in the NIR was most prominent. Held against the above findings from a tundra snow pack, this indicates that satellite-derived monitoring of broad-band albedo profits, at least for thin snow packs, from accounting for different spectral signatures for snow on land compared to snow on sea ice.

On the sea ice, even a thin snow layer (<20 cm) blocks out almost all solar radiation that otherwise would had been available for melting of sea ice and for absorption by the water masses beneath it. Undoubtedly, the snow-cover distribution plays a crucial role for solar energy-transfer between the atmosphere and the sea ice-ocean system; being important for marine biota production as well as in a climate context. For example, stratification due to sea-ice melt is known to trigger the bloom of phytoplankton production. Recently, an observed decrease in sea-ice extent and sea-ice thickness in the Arctic Ocean has received much attention (*e.g.* Rothrock *et al.*, 1999). These changes have to a large extent been attributed to an increase in air and/or ocean temperature. In addition, we think it is important to study precipitation patterns (*i.e.*, snow distribution) and changes in these in time and space and their effect on sea-ice thickness-distribution. In a climate regime where snow is absent only for about 3 months per year a change in snow thickness followed by a change in the timing of snow melt and disappearance will have a major effect on the amount of radiation available for sea-ice melt.

Finally, we would like to emphasise the need for improving the present relatively simple parameterisation of snow albedo in climate models. With the existing comprehensive observational data and models of the spectral-reflectance behaviour of snow combined with the improved monitoring capabilities provided by new satellite instruments, more realistic surface albedo should be used as input in future climate model-simulations.

Acknowledgments

We are grateful for fieldwork assistance by A. Blanco (University of Oulo, Finland), J. Boike (Alfred Wegener Institute, Potsdam, Germany), K. Sand (The University Courses on Svalbard, Longyearbyen), O.-G. Støen (Norwegian Polar Institute), personnel from the Norwegian Polar Institute's Research Station in Ny-Ålesund and personnel onboard the Russian icebreaker Akademik Federov. The Arctic and Antarctic Research Institute, the Norwegian Polar Institute, the Norwegian Research Council, and the NATO (CLG Grant No. EST.CLG.975781) are acknowledged for their funding support.

References

Barry, R.G. (1996): The parameterisation of surface albedo for sea ice and its snow cover. Progr. Phys. Geogr., **20**, 63–79.

Brandt, R.E. and Warren, S.G. (1993): Solar-heating rates and temperature profiles in Antarctic snow and ice. J. Glaciol., **39**, 99–110.

Curry, J.A., Schramm, J.L. and Ebert, E.E. (1995): Sea-ice albedo climate feedback mechanisms. J. Climate, **8**, 240–247.

Gerland, S., Winther, J-G., Ørbæk, J.B. and Ivanov, B. (1999a): Physical properties, spectral reflectance and thickness development of first year fast ice in Kongsfjorden, Svalbard. Pol. Res., **18**, 275–282.

Gerland, S., Winther, J-G., Ørbæk, J.B., Liston, G.E., Øritsland, N.A., Blanco, A. and Ivanov, B. (1999b): Physical and optical properties of snow covering Arctic tundra on Svalbard. Hydrol. Proc., **13**, 2331–2343.

Gerland, S., Liston, G.E., Winther, J-G., Ørbæk, J.B. and Ivanov, B. (2000): Attenuation of solar radiation in Arctic snow: field observations and modelling. Ann. Glaciol., **31** (in press).

Grenfell, T.C. and Warren, S.G. (1999): Representation of a nonspherical ice particle by a collection of independent spheres for scattering and absorption of radiation. J. Geophys. Res. **104**, 31697–31709.

Grenfell, T.C., Perovich, D.K. and Ogren, J.A. (1981): Spectral albedos of an alpine snowpack. Cold Reg. Sci. Tech., **4**, 121–127.

Grenfell, T.C., Warren, S.G. and Mullen, P.C. (1994): Reflection of solar radiation by the Antarctic snow surface at ultraviolet, visible and near-infrared wavelength. J. Geophys. Res., **99**, 18669–18684.

Hall, D.K., Riggs, G.A. and Salomonson, V.V. (1995): Development of methods for mapping global snow cover using moderate resolution imaging spectroradiometer data. Rem. Sens. Environ., **54**, 127–140.

IPCC TAR (2001): Intergovernmental Panel on Climate Change (IPCC) Third Assesment Report (in press).

Knap, W.H. and Reijmer, C.H. (1998): Anisotropy of the reflected radiation field over melting glacier ice: Measurements in Landsat TM Bands 2 and 4. Rem. Sens. Environ., **65**, 93–104.

Liston, G.E. (1995): Local advection of momentum, heat, and moisture during the melt of patchy snow covers. J. Appl. Meteorol., **34**, 1705–1715.

Liston, G.E., Winther, J-G., Bruland, O., Elvehøy, H. and Sand, K. (1999): Below-surface ice-melt on the coastal Antarctic ice sheet. J. Glaciol., **45**, 273–285.

Perovich, D.K., Roesler, C.S. and Pegau, W.S. (1998): Variability in Arctic sea ice optical properties. J. Geophys. Res. **103**, 1193–1208.

Rothrock, D.A., Yu, Y. and Maykut, G.A. (1999): Thinning of the Arctic sea-ice cover. Geophys. Res. Lett., **26**, 3469–3472.

Schlatter, T.W. (1972): The local surface energy balance and subsurface temperature regime in Antarctica. J. Appl. Meteorol., **11**, 1048–1062.

Steffen, K. and Heinrichs, J. (1994): Feasibility of sea ice typing with synthetic aperture radar (SAR): Merging of Landsat thematic mapper and ERS-1 satellite imagery. J. Geophys. Res., **99**, 22413–22424.

Warren, S.G. (1982): Optical properties of snow. Rev. Geophys. Space Phys., **20**, 67–89.

Warren, S.G. and Wiscombe, W.J. (1980): A model for the spectral albedo of snow. II: Snow containing atmospheric aerosols. J. Atmos. Sci., **37**, 2734–2745.

Winther, J-G., Gerland, S., Ørbæk, J.B., Ivanov, B., Blanco A. and Boike, J. (1999): Spectral reflectance of melting snow in a high Arctic watershed on Svalbard: Some implications for optical satellite remote sensing studies. Hydrol. Proc., **13**, 2033–2049.

Wiscombe, W.J. and Warren, S. (1980): A model for the spectral albedo of snow. I: Pure snow. J. Atmos. Sci., **37**, 2712–2733.

(Received April 3, 2000; Revised manuscript accepted July 3, 2000)